



A SERS Approach for Rapid Detection of microRNA-17 in the Picomolar Range

Journal:	<i>Analyst</i>
Manuscript ID	AN-ART-04-2019-000653.R1
Article Type:	Paper
Date Submitted by the Author:	13-May-2019
Complete List of Authors:	Schechinger, Monika; Texas A&M University College Station, Biomedical Engineering Marks, Haley; Texas A&M University College Station, Biomedical Engineering Mabbott, Samuel; Texas A&M University College Station, Biomedical Engineering Choudhury, Mahua; Texas A and M University College Station, Irma Lerma Rangel College of Pharmacy Cote, Gerard; Texas A&M University College Station, Biomedical Engineering ; Texas A&M University System, Center for Remote Health Technologies & Systems



Analyst

ARTICLE

A SERS Approach for Rapid Detection of microRNA-17 in the Picomolar Range

Monika Schechinger,^a Haley Marks,^a Samuel Mabbott,^a Mahua Choudhury,^b and Gerard Cote^{'a,c}

8ujmwwReceived 00th January
20xx,
Accepted 00th January 20xx

DOI: 10.1039/x0xx00000x

www.rsc.org/

Epigenetic biomarkers are powerful tools for early disease detection and are particularly useful for elusive conditions like preeclampsia. Predicting preeclampsia at an early stage is one of the most important goals of maternal-fetal medicine. To this end, recent studies have identified microRNAs—such as microRNA-17—as early biomarkers for preeclampsia. Yet clinical applications are lagging, owing in part to the sensing challenges presented by the biomarkers' small size and complex environment. Surface enhanced Raman spectroscopy (SERS) is an emergent optical technique that is recognized for its potential to overcome these challenges. In this study, DNA functionalized nanoparticles were designed as probes to capture and quantify miRNA-17 in solution. SERS was used to determine the presence and concentration of miRNA-17 based on the formation of plasmonic nanoparticle aggregates. The miRNA-17 assay was tested at concentrations of 1 pM to 1 nM in both PBS and a representative complex biological sample. In both situations the assay was unaffected by non-complementary microRNA samples. These results demonstrate SERS's specificity and sensitivity for a new biomarker (miRNA-17) that may ultimately be used in a detection platform for early diagnosis of preeclampsia.

INTRODUCTION

Preeclampsia is a placental disorder¹ which results in 70,000 maternal deaths and over 500,000 foetal deaths each year,² impacting around 5–8% of all pregnancies.³ It is a systemic disease characterized by diminished blood flow to the uterine, maternal hypertension, decreased placental-vascular endothelial activity, and coagulation. However, its etiopathogenesis is still largely unknown.⁴

Physicians most commonly diagnose preeclampsia late in gestation when symptoms manifest (around the 20th week) by documenting hypertension or proteinuria in an expectant mother.⁵ Routine check-ups are necessary since symptoms vary and resemble many common side effects associated with a healthy pregnancy. However, no preventative testing is currently available and treatment is nominal.⁵ Physicians actively administer antihypertensives or steroids to mitigate adverse health impacts.⁶ However, the only "cure" for preeclampsia is the delivery of the placenta and foetus, at which time all symptoms subside.¹ Early detection of preeclampsia through biomarkers thus may enable closer monitoring of

women at increased risk for developing preeclampsia and help identify candidates for participation in early intervention.⁷

Recently, several studies have identified potential epigenetic biomarkers that detect preeclampsia prior to its onset.^{8,9} In our earlier clinical study, we observed a rise in microRNA-17 (miRNA-17) concentration in the blood of preeclamptic mothers when compared to the blood of healthy mothers. In preeclamptic mothers, this increase in miRNA-17 occurred around 9th to 11th week of gestation.¹⁰ Likewise, a recent publication also found that miRNA-17 is also upregulated in placenta of preeclamptic mothers.¹¹ Currently, we cannot conclude that increases in miRNA-17 concentration are solely attributed to the onset of preeclampsia. Based on our clinical study and the pathway analysis for preeclampsia, we decided to use miRNA-17 as a prototype biomarker to create a detection assay for preeclampsia.

The biomarker, miRNA-17, is part of a class of non-protein coding nucleic structures between 19–23 nucleotides long that plays a salient role in gene expression.^{12,13} In particular, the ability of miRNAs to exist in stable clusters outside the cell makes them attractive tools for disease diagnosis.¹⁴ However, miRNAs exist at low relative concentrations in the blood, urine, and saliva and corresponding isolation and detection difficulties have stymied the use of miRNA testing in clinical diagnosis.^{15,16}

Traditional research techniques for isolating and examining miRNA from biological samples that are not suitable for the point-of-care include microarray, northern blotting, and reverse transcription-polymerase chain reaction (RT-PCR).¹² In practice, both microarray and northern blotting profiling techniques are used for samples with miRNA concentrations within the nM to

^a Texas A&M University, Department of Biomedical Engineering, 5045 Emerging Technologies Building, College Station, Texas, 77843

^b Texas A&M University, Irma Lerma Rangel College of Pharmacy, Reynolds Medical Building, College Station, Texas 77843

^c Texas A&M Engineering Experimentation Station, Center for Remote Health Technologies & Systems, 1041 Emerging Technologies Building, College Station, Texas 77843

*Electronic Supplementary Information (ESI) Available: nanoparticle characterization data; experimental information for SERS signal analysis; LOD calculations; statistical analysis; and ANOVA regression analysis.

pM range. RT-PCR has a lower detection limit and is used to profile miRNA at fM concentrations.¹⁷

Notably, miRNA makes up approximately 0.01% of the total RNA sample concentration in serum. This low concentration makes isolation and extraction of miRNA challenging, which may lead to inconsistent data and false results.¹⁸ Consequently, miRNA expression is typically defined based on relative changes and normalization of the cycle threshold.¹⁹ Furthermore, unknown data normalization methodologies, when combined with inconsistent reports for the concentration of circulating miRNA in blood and plasma, make determining a detection range challenging.²⁰⁻²²

As such, researchers are currently investigating several alternative miRNA detection platforms, including the use of nanoparticles, biological molecular-based sensing, locked nucleic acid (LNA) sensing, and chemical sensing.¹² Chemical assays are particularly attractive for sensing applications because they provide high-precision analytical results when combined with sensitive spectroscopic techniques like Raman spectroscopy.²³ The use of miRNA for early disease detection, particularly for preeclampsia, is lacking, but surface enhanced Raman spectroscopy (SERS) is potentially capable of overcoming difficulties with isolating and detecting miRNA at low concentrations.

Raman spectroscopy is a form of inelastic light scattering that produces unique “molecular fingerprint” spectra. However, Raman scattering is a rare phenomenon that naturally occurs in only one out of every one to ten million photons of light that undergo normal elastic scattering.²⁴ In order to increase the Raman signal, modern sensing applications often use metallic nanoparticles to create high-energy plasmonic ‘hotspots’ that increase the likelihood of photons to undergo Raman scattering, a process known as surface enhanced Raman spectroscopy (SERS).²⁵ SERS, therefore, provides an enhancement factor of $\sim 10^6$.²⁶ In this study, we describe a SERS detection technique that uses nanoparticles and a sandwich assay design.

EXPERIMENTAL

Materials and Instrumentation

The following chemicals were purchased from Sigma Aldrich: hydroxylamine hydrochloride, sodium hydroxide, silver nitrate, Tris (2- carboxyethyl) phosphine hydrochloride (TCEP), sodium chloride, potassium chloride, sodium phosphate, potassium phosphate, citric acid, sodium citrate, and hydrochloric acid. 3K Nanosep® Centrifugal Devices with Omega™ Membranes were purchased from Pall Corporation and used for desalting and concentrating oligonucleotide probes. Using the known sequence for miRNA-17, Integrated DNA Technologies synthesized the resulting 23-base-pair target RNA strand. Integrated DNA Technologies also synthesized 2 short strands of single-sided DNA (ssDNA) to be used for capturing target.

A Zetasizer Nano ZS90 (Malvern, UK) was used to determine nanoparticle size and zeta potential. The nanoparticle size was confirmed using a transmission electron microscope (TEM)

(FEI). Additionally, the function of the nanoparticle detection assay, with respect to aggregate formation due to the addition of miRNA-17, was examined using TEM images of the assay combined with target miRNA-17. The relative concentrations of the nanoparticles, probes, target, and relevant combinations were calculated using Beer-Lambert’s Law based on known extinction values and the absorbance values (Fig. S1†) collected with an Infinite® 200 Pro multimode microplate reader (Tecan, Switzerland). The SERS signal was observed using a ThermoScientific DXR Raman confocal microscope (10x NA, 900 g/mm grating, 532 nm Excitation Wavelength, 10 mW). The resultant SERS spectra provided resulted from the average of 5 spectra with each spectrum consisting of the average of 10 consecutive 1 s scans.²⁷

Synthesis and Characterization of Silver Nanoparticle Colloid

Silver colloid was synthesized using a similar method to that originally developed by Leopold and Lendl.²⁸ While under vigorous stirring, 1 mL of hydroxylamine hydrochloride ($\text{NH}_2\text{OH}\cdot\text{HCl}$, 167 mM) was added to 89 mL of sodium hydroxide (NaOH , 33.3 mM). Ten mL of silver nitrate (AgNO_3 , 10 mM) solution was then rapidly added to the solution, and the solution was left stirring for 15 minutes at room temperature.

Nanoparticle Functionalization

The approach for nanoparticle functionalization and labelling was adapted based on the protocol previously described by Schechinger et al.²⁷ The oligonucleotide probes were designed with a THIOL end modification which allowed the probe to be immobilized on the nanoparticle surface. Briefly, the oligonucleotide solution of ssDNA labelled as Probe 1 was reduced by combining 100 μL of 20 mM TCEP with 100 μL of the oligonucleotide solution (100 μM). The sample was then left at room temperature for 60 minutes. Next, the solution was subjected to 3 consecutive wash cycles using a desalting column (3kDa, Nanoseps) to remove existing reaction byproducts and TCEP in solution. For each cycle, the desalting column containing the sample was centrifuged (5 minutes at 5.0 rcf (rotational centrifugal force)). The filtered waste was then removed from the bottom of the collection tube and 300 μL of suspension solution was added to the top of the desalting column. The first 2 wash cycles used deionized distilled water (DDW) as the suspension solution. For the third and final wash, 0.3 M phosphate buffer saline (PBS) solution (pH 7.4) was used. The sample was then collected and stored in 0.3 M PBS hybridization buffer. This procedure was repeated using the Probe 2 oligonucleotides.

The value for the number of immobilized oligonucleotides on the surface of a single nanoparticle used during nanoparticle functionalization was set at 1500 oligos/NP. Beer-Lambert’s Law was used to calculate the concentration of each sample of reduced oligonucleotide using the extinction coefficients and absorption maxima of each probe as provided by IDT.

Next, 1 mL of silver nanoparticles (AgNPs) was placed in a new vial. The calculated volume of Probe 1 was added to the vial, and the sample was left to shake overnight for approximately 8 hours. The following morning, a 250 mM

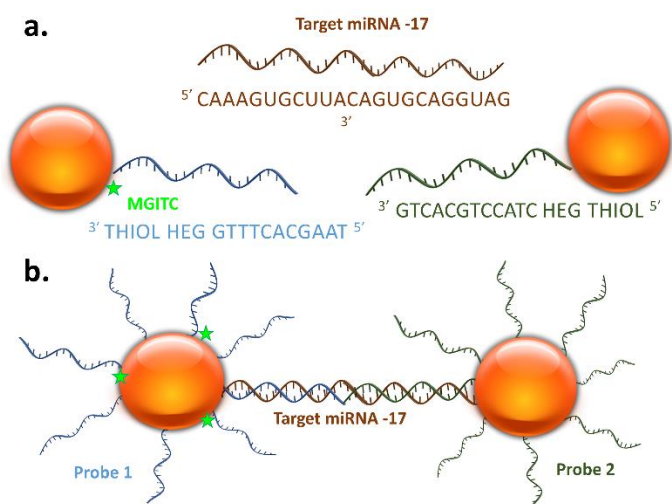


Fig. 1 Basic overview of a) the sandwich assay design for miRNA-17 showing the individual probes and b) the resultant binding of miRNA-17 with the nanoparticles.

solution of citrate/HCl buffer (pH 3) was prepared and used to promote complete coverage of the nanoparticle surface. Citrate buffer (20 μ L) was added to the AgNPs/DNA solution and then shaken for a few seconds. This process was repeated 3 times, adding a total of 60 μ L of citrate solution to each sample. The sample was left shaking for 20 minutes and then centrifuged (20 minutes at 3.3 rcf).²⁹ The supernatant was collected and discarded, thereby removing any free-floating oligonucleotides. The remaining pellet, formed at the bottom of the tube, was re-suspended in PBS buffer (pH 7.4). The same process was carried out for Probe 2.

Labelling using Raman Dye

Following functionalization, the solution of nanoparticles (sol) coated with Probe 1 was labelled using the photoactive dye, malachite green isothiocyanate (MGITC). No dye was added to nanoparticles functionalized with Probe 2. The value of dye molecules bound to each nanoparticle was set at 1000. The appropriate volume of dye was calculated and then added to the 1 mL sol functionalized with Probe 1. The sample was left to shake for 1 hour and then set aside to react overnight (~8 hours) at room temperature. The following morning, the sample was centrifuged (20 minutes at 3.3 rcf) and the supernatant was discarded, thereby removing the excess unreacted dye in solution. PBS buffer (pH 7.4) was then used to re-suspend the remaining nanoparticle pellet.

Oligonucleotide-Nanoparticle Probe for miRNA-17

A sandwich assay incorporating the nanoparticle probes was designed for the selective capture of miRNA-17.³⁰ This design consisted of two probes—Probe 1 (Sequence: 5' TAA GCA CTT TG HEG THIOL 3') and Probe 2 (Sequence: 5' THIOL HEG CTA CCT GCA CTG 3')—each complementary to half of the target miRNA-17 strand (5' CAA AGU GCU UAC AGU GCA GGU AG 3') (Fig. 1). THIOL and hexaethylene glycol (HEG) modifiers were added to enable the oligonucleotide probes to attach to nanoparticle surfaces. The binding of thiolated oligonucleotide probes on the

nanoparticle surface was confirmed by a slight redshift in the localized surface plasmon resonance (LSPR) or maximum peak in the absorption spectra (Fig. S1[†]). This small LSPR shift is due to an increase in the refractive index at the surface of the nanoparticle following the binding of the oligonucleotide probes.³¹ The nanoparticle size was defined based on the absorption maximum at 408 nm and was then confirmed as ~35 nm using TEM images (Fig. S2[†]).

The assay was engineered to enable the conjugated nanoparticles to remain suspended and stable in a physiological buffer solution (0.3 M PBS, pH 7.4) similar to blood plasma. The zeta potential, a parameter related to surface charge, is typically used for understanding nanoparticle stability. The effective surface charge is key to maintaining necessary electrostatic interactions that support the colloid suspension. A negative surface charge is typical of hydroxyl amine reduced metallic nanoparticles, like silver, due to the presence of orientation of the molecules that results in hydroxyl groups at their surface. These negatively-charged surface ions provide the electrostatic repulsion to sustain the colloid.³² The zeta potential of both the functionalized nanoparticle solutions was around -32 mV.³³

The combined sol with Probe 1 and nanoparticles with Probe 2 produces the diagnostic assay. As described, the assay avoids premature nanoaggregate formation due to the incompatible base pairing and orientation sterics of the two probes will form a dsDNA complex. Upon addition of the target miRNA-17 strand, nanoaggregates form, as particles from the Probe 1 and Probe 2 populations bind to the same strand of miRNA-17. The high affinity between DNA and miRNA overcomes the repulsion of negatively charged nanoparticles, bringing particles close enough together to allow for their individual plasmons to couple. This generates 'hot spots' of increased SERS intensity at the particle gaps where the Raman reporter probe is located³⁴, on the order of 10^3 for this specific assay (Fig. 2). TEM images of the plasmonic nanoparticles aggregates resulting from the addition of miRNA-17 are provided in the supplementary information (Fig. S3[†]).

Analysis of the SERS Assay's Response to miRNA-17 Presence

MGITC was used as the Raman reporter molecule to indirectly sense the target analyte, miRNA-17. This was performed by examining changes in the analyte's relative SERS intensity, which increases as a function of nanoaggregate formation. The area of known peaks at Raman wavenumbers of 1177 cm^{-1} , 1220 cm^{-1} , 1290 cm^{-1} , 1586 cm^{-1} , and 1618 cm^{-1} were used to define the relative SERS intensity observed for different target concentrations. The Integrate Peak function in Origin Lab was used to calculate the peak area.

To reduce instrumental noise, Savitzky-Golay smoothing was applied.³⁵ The calculated values were plotted alongside their prospective target concentrations and then fit with a Hill curve. The curve was used to obtain a representative linear lookup table describing the relationship between the target concentration in solution and the observed relative SERS intensity. The limits of detection (LOD) and coefficient of determination were calculated to determine the lowest concentration that can be distinguished from a PBS blank.

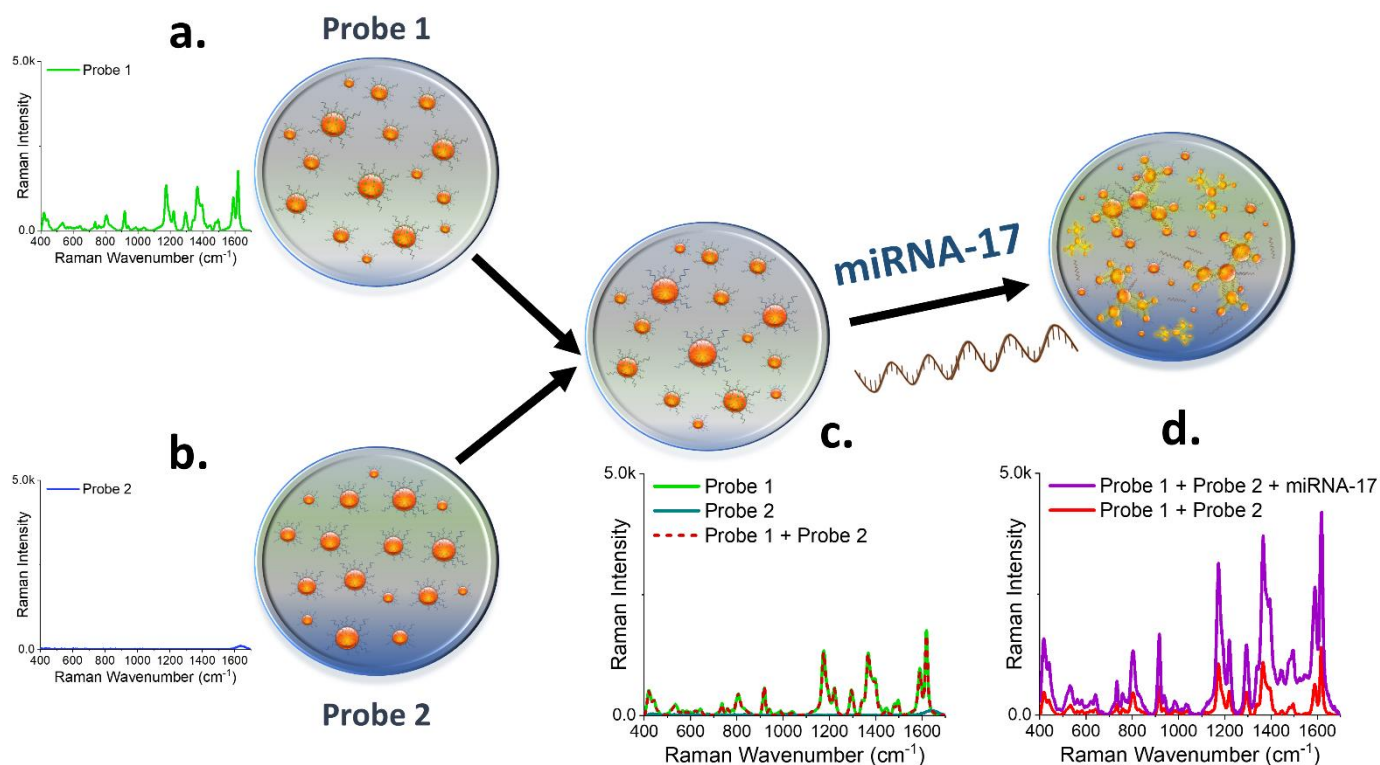


Fig. 2 Representative SERS spectra of the assay nanoparticles: (a) Probe 1 provides a visible SERS spectra from its MGITC reporter dye; (b) Probe 2 lacks any discernible signal thereby demonstrating the DNA probes do not contribute to the spectra; (c) the combined miRNA-17 assay solution combining nanoparticle Probe 1 + Probe 2, which produces no change in the signal indicating no nonspecific DNA hybridization occurs between probes; (d) the assay response upon the addition of miRNA-17, which causes an increase in the SERS signal due to the formation of aggregates resulting from DNA-RNA hybridization.

To determine the selectivity of the assay, 10 pM of a non-complementary strand of miRNA was added to the assay in lieu of miRNA-17. The resultant SERS spectra were analysed and compared to the corresponding sample containing miRNA-17. This process was performed for 5 different non-complementary negative control strands: miRNA 34a-3p, miRNA 126a-3p, miRNA 155-3p, miRNA 210-3p, and U6.

Evaluation of SERS Assay in a Complex Biological Sample

The designed nanoparticle detection assay for miRNA-17 was further evaluated in diluted bovine serum to determine its functionality within a complex biological sample. The bovine serum was isolated from whole bovine blood, provided by College of Veterinary Medicine, by centrifuging the sample at 1.3 rcf for 10 minutes and collecting the supernatant. The supernatant (serum) was then diluted to 20% (v/v) in 0.3M PBS. The Raman spectra of the diluted serum solution was then collected with a 532 nm excitation laser using the same collection parameters previously described. The individual assay components along with the combined sensing assay were each mixed with diluted bovine serum. The three samples were then incubated at room temperature. After 1 hour, the SERS spectra of the different reference solutions were collected.

The designed sensing assay was further tested to confirm its quantitative capacity for miRNA-17 within bovine serum. The diluted bovine serum was doped with different concentrations of the target, miRNA-17. The assay components were combined

with the target suspended in diluted bovine serum and incubated at room temperature for 1 hour. The SERS signal was then collected and analysed based on the previous methods.

To contribute to the complexity of the biological medium, the diluted bovine serum was doped with a non-complementary oligonucleotide strand in addition to the target miRNA-17. The non-complementary strand was chosen based on the results of the assay specificity study in PBS. In accordance with the earlier study, a concentration of 10 pM was used for both the target miRNA-17 and non-complementary oligonucleotide strand. The resulting SERS spectra was then compared to data obtained from the assay combined with 10 pM of miRNA-17 in PBS and diluted bovine serum. In order to determine the presence of miRNA-17 prior to doping, the diluted bovine serum was analysed using real-time reverse transcription PCR (qRT-PCR).

RESULTS AND DISCUSSION

Proof of Concept for Detection of miRNA-17 using SERS

The robustness of assay was first tested in PBS by individually examining the baseline SERS spectra of the two assay components— AgNPs functionalized with Probe 1 and labelled with MGITC, and AgNPs functionalized with Probe 2 only (Fig. 2). The solutions were then combined and the SERS spectrum was collected and designated as the reference spectrum.

Upon further examination, the SERS spectra of the combined sensing assay had a maximum signal intensity comparable to that of the sol with Probe 1. This was as expected, indicating that there is no nonspecific binding between the probes when no miRNA is present. The sol with Probe 2 had a negligible signal due to the absence of a Raman reporter molecule, thus validating that there is no contribution to the spectra from the DNA probes themselves.

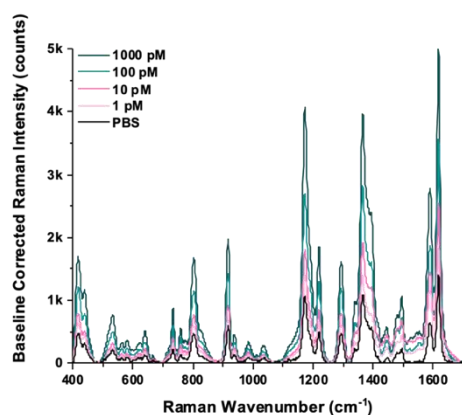
The combined sensing assay was then further analysed with the addition of 1 nM of miRNA-17. A previous study revealed that a 1-hour incubation or reaction time was required for the assay to reach steady-state—as indicated by a stable SERS maxima.²⁷ The SERS spectra for the sensing assay with 1 nM of miRNA-17 was obtained following this incubation period. The resultant spectra had a notably higher maximum relative SERS intensity, thus suggesting hybridization of the target miRNA and oligonucleotide probes by way of formation of aggregates (Fig. 2). These findings indicate the assay's potential to successfully detect the presence of miRNA-17. To avoid particle saturation the assay was optimized based on the sensing criteria and the necessary detection range for miRNA-17.

Quantification of miRNA-17 using Normalized SERS

The nanoparticle assay as described was then used to determine the quantitative capacity of MGITC to indirectly sense for miRNA-17 in both PBS and serum. The assay was first tested in PBS without the presence of non-complementary competing analytes. The SERS intensity of the assay was examined for different concentrations of miRNA-17 ranging from 10 fM to 10 nM (Fig. S4[†]). As discussed in the previous section, a visible jump in the relative SERS intensity occurs when miRNA-17 is added and appears at first glance to be concentration dependent in the range of 1 pM - 1 nM. The spectra displayed represent the mean of three individual replicates gathered for each incremental miRNA-17 concentration. The signal was baseline corrected prior to peak analysis using asymmetric least squared smoothing (Fig. 3).³⁶

The overlay of the average spectra obtained for the various sample concentrations in Figure 3 visually suggests a possible relationship between target concentration and SERS intensity.

Fig. 3 Baseline-corrected SERS spectra of the nanoparticle assay in response to 1 pM - 1 nM miRNA-17, demonstrating the concentration dependence of the assay.



The largest relative SERS intensity was observed when at least 1 nM of miRNA-17 was present. Additionally, as the amount of miRNA in solution decreased to less than 1 pM, the decreases in relative SERS intensity became negligible. This same general trend was observed by Graham et al for a DNA-DNA hybridization assay suspended in PBS.²⁹ Thus, initial results indicate that the designed scheme may be altered to suit various nucleic acid and biomarker conformations.

Multiple Peak Analysis of SERS Signal to Determine LOD

To more closely study the relationship between target concentration and the resultant SERS signal, the relative SERS intensity was defined by calculating the peak area for multiple characteristic peaks associated with MGITC. The characteristic peaks chosen were centred at 1177 cm⁻¹, 1220 cm⁻¹, 1290 cm⁻¹,³⁷ 1586 cm⁻¹, and 1618 cm⁻¹³⁸ (Table 1). These peaks are commonly used to analyse the SERS spectra of MGITC, and they also help avoid overlap peaks from common interference from blood located in the fingerprint region, such as aromatic rings (828, 872, 1000, 1110, 1204, 1546 cm⁻¹), methylene vibrational modes (1266, 1320, 1365, 1449 cm⁻¹), carboxylic group vibrations (620, 964, 1397, 1584 cm⁻¹), stretching of disulphide bonds (500 - 550 cm⁻¹ and 650 - 675 cm⁻¹), and α -helical secondary structures (890-960 cm⁻¹).³⁹

The average area calculated for each chosen peak was then binned by peak location as a function of concentration (error bars correspond to 1 standard deviation) (Fig. 4). Before normalization, the peaks at 1177 cm⁻¹ and 1618 cm⁻¹ provided the largest relative SERS intensity when examined across different miRNA-17 concentrations and thus would be expected to provide the lowest LOD, whereas the peaks with weaker relative SERS intensity were associated with the peaks centred at 1220 cm⁻¹ and 1290 cm⁻¹. Interestingly, when normalized to the control spectra (e.g., assay without any miRNA, labelled PBS only), all peak locations exhibited a similar concentration dependence (Fig. 4b), but the lowest LOD was associated with the less obvious peak at 1586 cm⁻¹.

The limit of detection (LOD) is calculated based on the intensity limit determined at each peak. The Intensity Limit (I_{LIMIT}) was calculated based on the average SERS intensity and standard deviation compared to the PBS reference.³⁵ The target concentration associated with the calculated I_{LIMIT} was determined using a representative equation for predicting miRNA-17 concentrations from relative SERS intensity. The LOD ranged from 0.16 pM (Peak at 1586 cm⁻¹) to 0.91 pM (Peak at 1220 cm⁻¹) (Table S1[†] and S2[†]).

Table 1 Vibrational Peak Assignment for Five Characteristic Peaks of MGITC

RAMAN PEAK (cm ⁻¹)	SERS PEAK (cm ⁻¹)	VIBRATIONAL ASSIGNMENT
1176	1177	In-Plane C-H Bend, Benzene ν_9 Mode
1221	1220	N-C Stretch, NR ₂ Bend
1295	1290	In-Plane C-H and C-C-H
1590	1586	Stretch/Bend of In-Plane Ring
1619	1618	Stretch of C-C and N-Phenyl Ring

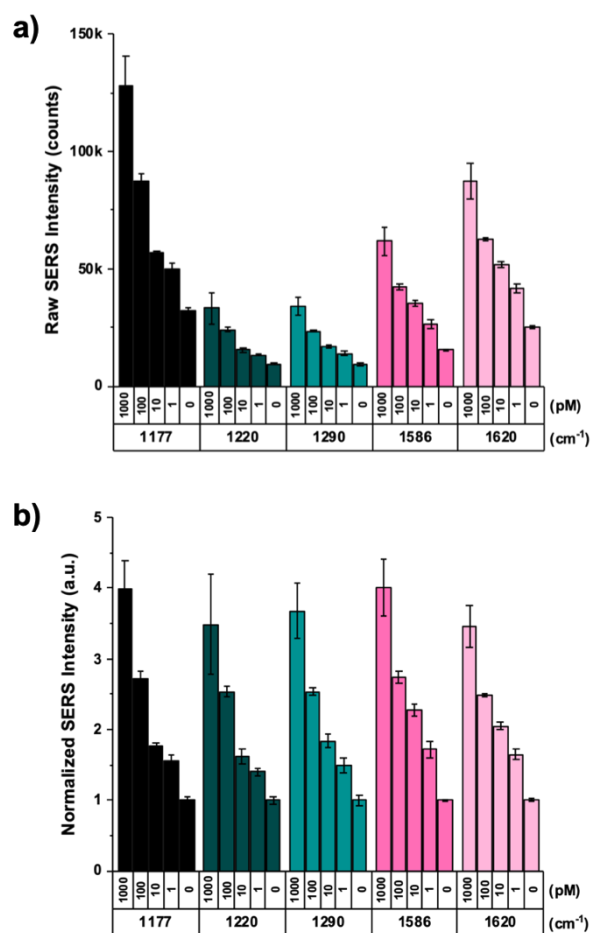


Fig. 4 Bar graphs defining the a) peak area SERS intensity at five characteristic peaks of MGITC for various miRNA-17 concentrations; b) the data for the peak area SERS intensity normalized to PBS.

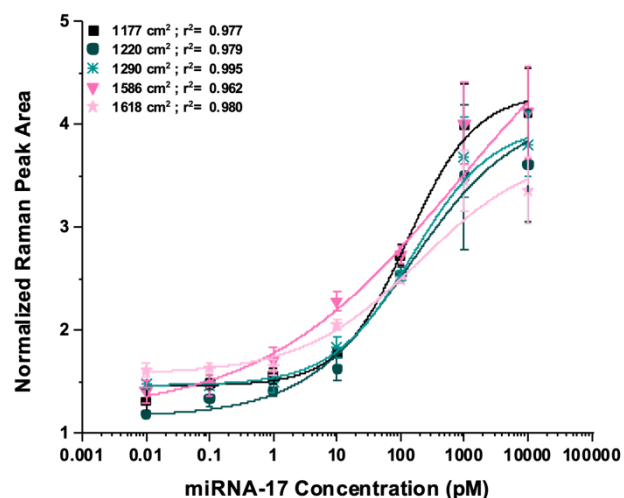
Evaluation of SERS Detection Assay Dose-Response Curves to Determine Variations in Relative Binding Avidity & Dynamic Range

The data was replotted using a scatter plot and fit to a curve to better visualize the relationship between peak area and target concentration. Across data sets, a similar general sigmoidal dose-response was observed corresponding to different locations of the peak centre, thereby signifying coherence in the assay response regardless of which peak is analysed. Data was then fit to a dose-response curve using the Hill1 equation in Origin Pro (Fig. 5). From these fits, we observed an effective dissociation constants of 129 pM, 143 pM, 155 pM, 756 pM, and 195 pM for the peaks centred at 1177 cm⁻¹, 1220 cm⁻¹, 1290 cm⁻¹, 1586 cm⁻¹, and 1618 cm⁻¹, respectively (Table S3⁺). The values for the dissociation constant and Hill coefficient (*n*) are provided alongside the calculated statistical fit (coefficient of determination (COD) and adjusted R²) for the Hill1 equation for five characteristic peaks of MGITC whose intensity is associated with the miRNA-DNA binding event. The apparent dissociation

constant, *K_d*, describes the affinity between the target analyte for the capture probes, and in turn relates to the sensitivity of the assay. A higher binding affinity corresponds in an increase in the sensitivity of the detection assay.⁴⁰ A Hill coefficient (*n*) of less than 1 signifies negative cooperativity in which the binding of a ligand (miRNA-17) to a receptor (capture probes) decreases the binding affinity of subsequent receptors.⁴¹ All five characteristic peaks produced a Hill coefficient of less than 1, indicating that the assay exhibits negative cooperativity, as expected due to steric hindrance caused by the dense packing of ligands on the nanoparticle surface. However, it is worth noting that, depending on the peak being analysed, this value ranges significantly from 0.284-0.820, despite being derived from the same binding event. This thus highlights the importance of multi-peak analysis and peak choice in the design of SERS assays with a single reporter molecule. Ultimately, the Hill coefficients were used to define a representative equation relating SERS signal intensity with miRNA-17 concentration (Equation S3⁺).

Paired t-tests ($\alpha = 0.05$) were used to determine if the samples tested could be differentiated with 95% confidence (Table S4⁺ and S5⁺). The peak centred at 1618 cm⁻¹ was chosen to perform these tests because it had the best linear fit in the 1 pM - 1 nM range (Table S6⁺). The signal for each miRNA-17 concentration tested was differentiable with 95% confidence from the baseline signal for the assay with PBS, without any correction factors applied. However, the signal was not differentiable at the highest (10 nM and 1 nM) and lowest target concentrations (1 pM, 100 fM, and 10 fM) tested. Therefore, the range of quantification for the designed assay was determined to exist from 1 pM to 1 nM, as was expected by our earlier visual assessment of the spectra.

Fig. 5 The semi-log plot of the peak area for the characteristic peaks of MGITC (1177 cm⁻¹, 1220 cm⁻¹, 1290 cm⁻¹, 1586 cm⁻¹, and 1618 cm⁻¹) fit to the Hill1 equation.



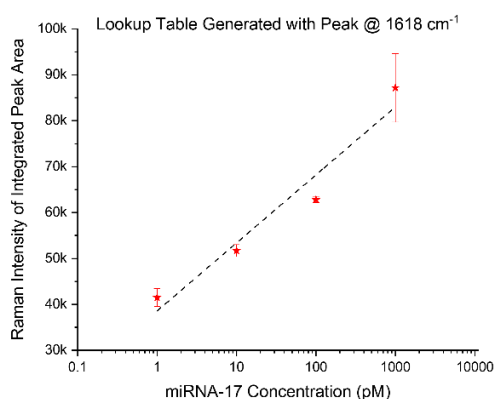


Fig. 6 The semi-log plot with the representative logarithmic equation $I = 1.48E4 * \log(x) + 2.16E5$, where x is the concentration in pM and I is the SERS intensity in counts using the peak centred at 1618 cm^{-1} .

A strong logarithmic fit was observed across all peak locations, irrespective of which peak was used to generate the calibration curve. That is, a statistically significant relationship between the relative SERS intensity and the concentration of the target miRNA-17 was observed at a significance level, α , of 0.05. Thus, the equations for each dataset have high predictive value. The linear regression for the peak at 1618 cm^{-1} was the most statistically significant. It provided the highest values for the correlation coefficient ($R = 0.975$) and the smallest p-value ($p = 0.0253$).

Additionally, this peak's calibration curve showed the second strongest raw SERS intensity, thus making it easily detectable in post processing. Given these superior characteristics, the data collected from this peak were used to develop a representative lookup table for predicting miRNA-17 concentrations from relative SERS intensity (Fig. 6). Linear regression analysis for the peak at 1618 cm^{-1} resulted in the following representative logarithmic equation: Intensity = $1.48E4 \log(\text{Concentration}) + 2.16E5$. A summary of the figures of merit, which includes parameters typically used for analysing SERS assays, is provided in Table 2. While the results provided in Table 2 represent the overall performance of the designed SERS biomarker detection assay, they are predicated on the peak centred at 1618 cm^{-1} .

The significance of the peak location for SERS signal intensity was further examined using descriptive statistics and one-way ANOVA. Using a significance level (α) of 0.05, ANOVA analysis determined that Raman peak location significantly influenced the SERS signal intensity (Table S7[†]). This information substantiates the data obtained using regression analysis, as demonstrated by the variation in slope and intercept across peaks. Therefore, identifying a statistically significant peak is key in determining the relationship between signal intensity and concentration of the target analyte. A one-way ANOVA was also used to confirm the statistical significance of the relationship between miRNA-17 concentration and SERS signal intensity (Table S8[†]).

The figures presented in Table 2 indicate the potential of SERS as a diagnostic platform for the early detection of preeclampsia as compared to traditional techniques. The

PEAK AT 1618 cm^{-1}	
SENSITIVITY	1.48×10^4 (counts/pM)
LIMIT OF DETECTION (LOD)	0.26 pM
DYNAMIC RANGE (LOQ)	1 - 1000 pM
INTERCEPT (BASELINE INTENSITY)	2.16×10^5 (counts)
PEARSONS CORRELATION	0.975
p-VALUE FOR H_0 : SLOPE=0	0.0253

Table 2 Summary of figures of merit for the miRNA-17 detection assay

designed sensor has a lower LOD than both northern blotting and microarrays, and a comparable LOD to RT-PCR. This high degree of sensitivity and quantitative capacity makes a SERS-coupled nanoparticle detection assay an attractive alternative to current laboratory techniques. Indeed, the designed SERS assay reliably produces quicker results than traditional methods because it requires fewer steps.

Specificity of miRNA-17 Assay

The specificity of the assay for sensing miRNA-17 was determined using 4 different non-complementary strands of miRNA (34a-3p, 126a-3p, 155-3p, 210-3p) and a small strand of non-coding nuclear RNA (U6). A 10 pM concentration of each of the non-complementary strands was added to the assay in place of the complementary strand (miRNA-17). Once again, spectra analysis was performed by calculating the total area for the characteristic SERS peaks centred at 1177 cm^{-1} , 1220 cm^{-1} , 1290 cm^{-1} , 1586 cm^{-1} , and 1618 cm^{-1} (Fig. 7).

The combination of sensing assays with non-complementary target strands provided SERS spectra with low relative intensities comparable to that observed for the blank (Fig. 7). The low relative intensity indicates the absence of large aggregates that enhance the SERS signal; the SERS signal observed is most likely due to the localized surface plasmon effect. In comparison, the assay containing the complementary target, miRNA-17, produced drastically higher SERS intensity due to its potential to form aggregates with high energy "hot spots." Once again, the largest values for peak area were associated with the peaks centred at 1177 cm^{-1} and 1618 cm^{-1} , and the smallest peak areas were calculated for the peaks centred at 1220 cm^{-1} and 1290 cm^{-1} . Furthermore, paired t-tests ($\alpha = 0.05$) were used to determine the differentiability of the non-complementary strands from the baseline (Table S9[†]). The forward and reverse of the non-complementary strands were not differentiable with 95% confidence from the assay with PBS.

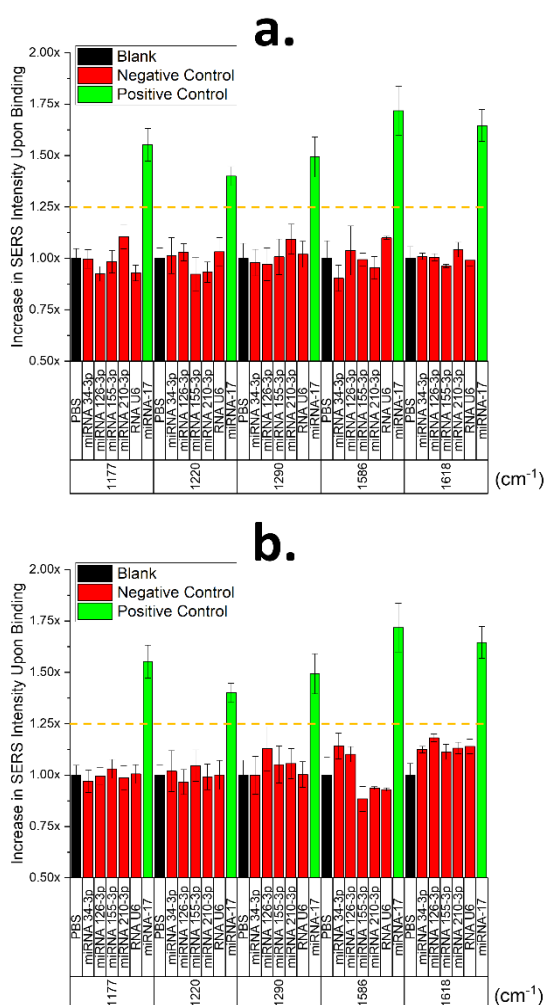


Fig. 7 Peak area normalized to PBS, of the various a) forward and b) reverse non-complementary strands of negative control RNA compared to the blank and positive control (target miRNA-17). In both scenarios, a threshold can be set at a signal intensity increase of 1.25x that of PBS.

Overall, the results collected using both complementary and non-complementary strands of miRNA indicate that the assay exhibits a degree of specificity for the target, miRNA-17. When the assay was introduced to similar strands of miRNA, the resultant signal fell below the LOD. Thus, based on the weak signals observed with the non-complementary strands of miRNA, a degree of selectivity within the assay can be inferred.

Analysis of SERS Assay in Complex Biological Medium

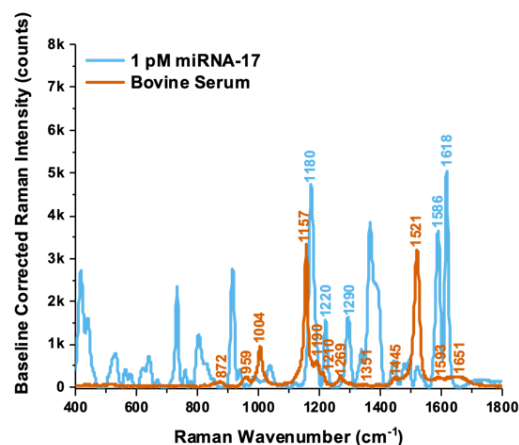
The designed nanoparticle detection assay was then tested using diluted bovine serum (20% v/v), a complex biological medium similar to human serum. The Raman spectra of the diluted bovine serum solution were first collected to determine the underlying baseline Raman signal present when testing the detection assay in serum (Fig. 8). The resulting spectra contained multiple characteristic peaks. These peaks exist because of the various biomolecules present in serum^{42, 43} (Table S10⁺). To determine potential peak overlap, the MGITC SERS signal for the detection assay with 1 pM of miRNA-17 was plotted alongside the Raman spectra for serum (Fig. 8). The resulting plot showed serum peaks, between 1000 cm⁻¹ to 1550

cm⁻¹, that could potentially influence the signal intensity of the 5 characteristic peaks of MGITC previously analysed. While none of the serum peaks directly coincided with the specific peaks examined for MGITC, some peak overlap did exist. This overlap primarily occurred for the MGITC peaks centred at 1180 cm⁻¹, 1220 cm⁻¹, and 1290 cm⁻¹, with the most overlap occurring at 1180 cm⁻¹. Before adding the designed nanoparticle detection assay, the bovine serum was analysed using qRT-PCR to determine if miRNA-17 was present in the sample. The results indicated that a small concentration of miRNA-17 did exist within the bovine serum sample (Fig. S5⁺). This underlying miRNA-17 concentration was referred to as the baseline signal (Fig. S6⁺).

The nanoparticle detection assay suspended in diluted bovine serum was analysed at various miRNA-17 concentrations (Fig. 9a). To ascertain the relationship between target concentration and signal intensity, the assay was tested from 10 fM to 10 nM (Fig. S7⁺). The same overall trend was observed as described above for PBS. However, the maximum signal intensity was collectively higher for the results collected in serum as compared to PBS. A comparison of the characteristic SERS spectra showed that the results from the assay in serum produced a more prominent peak at 1180 cm⁻¹ with a higher maximum signal intensity. This likely result from the underlying Raman signal of the serum solution and its existing peak overlap with the spectra for MGITC. Similarly, the integral for each of the five characteristic peaks of MGITC was calculated from the resultant spectra of the assay in serum. The calculated values for the integrated peaks once again resulted in a higher SERS intensity compared to the assay in PBS.

Due to the differences in the maximum signal intensity and the presence of an underlying baseline signal, further comparison was performed based on the normalized results of the assays (Fig. S8⁺). The results from the assay in serum were normalized to the control spectra: the Raman spectra of the assay in serum without the target analyte. The LOD was then calculated based on the normalized results of the integrated peak area (Table S11⁺). The values for the LOD calculated for assay in serum ranged from 0.22 pM (1586 cm⁻¹) to 2.89 pM (1220 cm⁻¹). Compared to the LOD for the assay in PBS, the assay

Fig. 8 Raman spectra of diluted bovine serum (20% v/v) with the significant peaks labelled, alongside the SERS spectra of the detection assay.



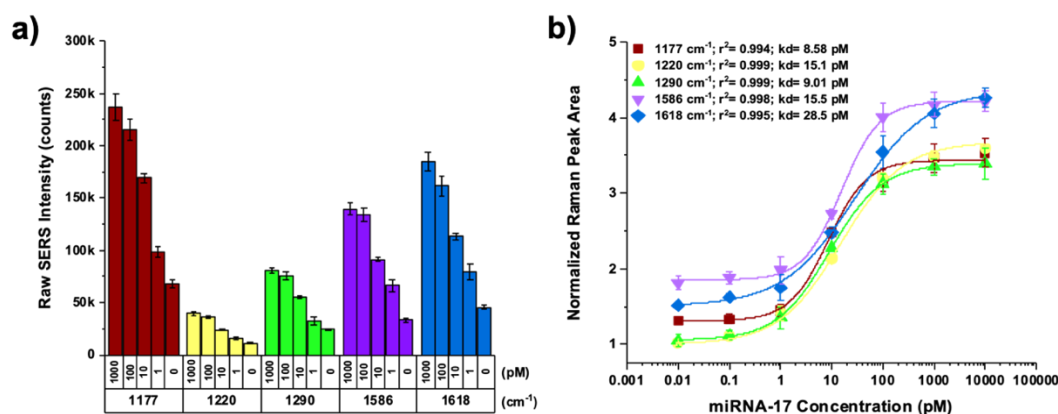


Fig 9 The (a) integrated peak area of the characteristic peaks of MGITC for the assay in diluted bovine serum and (b) the Hill1 fit for the relative equation of the characteristic peaks.

in serum produced slightly higher values for the LOD. When tested in complex solutions like serum, increases in the LOD have been reported for sensing assays with uncoated functionalized nanoparticles.^{44, 45} This increase is commonly attributed with serum-protein-induced dissociation of Raman reporter molecules and capture probes from the nanoparticle surface.^{46, 47} Thus, the observed increase in LOD for the assay in serum indicates some degree of dissociation of the reporter molecules and oligonucleotide probes from the nanoparticle surface.

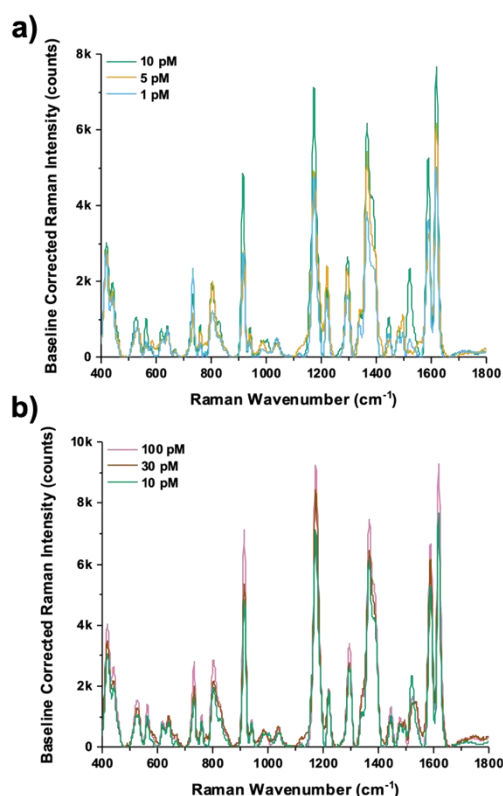
The normalized results of the integrated peak area from assay in serum were fitted to a Hill1 equation to establish a representative equation of the assay's sensing characteristics (Fig. 9b). The sensing parameters obtained from the Hill1 Fit include the dissociation constant and the Hill coefficient (Table S5[†]). As compared to the assay in PBS, the assay in serum produced lower values for the apparent dissociation constant obtained from the following peaks: 8.58 pM (1177 cm⁻¹), 15.1 pM (1220 cm⁻¹), 9.01 pM (1290 cm⁻¹), 15.5 pM (1586 cm⁻¹), and 28.5 pM (1618 cm⁻¹). A decrease in the k_d is related to an increased affinity for the target, miRNA-17.⁴⁸ The observed shift in the k_d is likely due to the dissociation of oligonucleotide probes from the nanoparticle surface, previously mentioned. The dissociation results in a decrease in the probe density on the nanoparticle surface, which for a fixed sample volume, is linked to the apparent k_d .⁴⁹

In addition to the dissociation constant, variation in the reported Hill coefficient, n , among the different peaks indicates changes in the detection assay's sensing efficiency when incorporated into a complex biological sample such as serum. At each peak examined, the Hill coefficient for the assay in PBS had a value of less than 1, indicating the assay exhibited negative cooperativity. Meanwhile, the assay in serum positive exhibited more variation in the Hill coefficient with the peaks at 1177 cm⁻¹ and 1586 cm⁻¹, resulting in values greater than 1 or cooperativity. The remaining peaks centred at 1220 cm⁻¹, 1290 cm⁻¹, and 1618 cm⁻¹ produced negative values for the Hill

coefficient. Therefore, the cooperativity for the assay in serum varied based on peak location so the overall cooperativity of the assay could not be determined.

The serum data was also subjected to linear regression analysis resulting in a logarithmic fit of the representative equation of the assay. Once again, the relationship between the SERS intensity and target concentration was determined to be statistically significant ($\alpha = 0.05$). Compared to predictive

Fig. 10 The test concentrations of (a) 5 pM and (b) 30 pM were plotted individually alongside the upper and lower concentrations used to obtain the representative equation.



	LINEAR REGRESSION ANALYSIS				HILL FIT			
	PBS		Bovine Serum		PBS		Bovine Serum	
	SERS Intensity	Concentration (pM)	SERS Intensity	Concentration (pM)	SERS Intensity	Concentration (pM)	SERS Intensity	Concentration (pM)
5 pM	1.02E+05	1.98E+04	1.02E+05	4.70	1.02E+05	Undefined	1.02E+05	5.02
30 pM	1.35E+05	3.58E+06	1.35E+05	37.77	1.35E+05	Undefined	1.35E+05	30.70

Table 3 Comparison of the representative equations calculated for assay in PBS and serum using both linear regression analysis and Hill fit.

equations derived from the assay PBS, the assay in serum yielded a stronger logarithmic fit at each of characteristic peaks (Table S6[†]). Specifically, the peak at 1618 cm⁻¹ had the highest R-value of 0.992 while also having one of the smallest p-value ($p = 0.0162$).

The competency of representative equations, derived from different curve fitting methods, was evaluated using the additional miRNA-17 concentrations of 5 pM and 30 pM. The resultant samples consisted of the detection assay suspended in separate solutions of diluted bovine serum doped with either 5 pM or 30 pM of miRNA-17. These samples were then used to assess the different representative equations obtained from both PBS and serum. The resultant SERS spectra were collected for both sample solutions. The equations were tested using the assay in serum and evaluated in regards to the peak at 1618 cm⁻¹. The resulting SERS spectra were obtained for the assay with 5 pM and 30 pM of miRNA-17 (Fig. 10). The peak at 1618 cm⁻¹ was chosen based on its superior overall fit. The integrated SERS intensity calculated for the two assays doped with 5 pM and 30 pM of target was 1.02×10^5 counts and 1.35×10^5 counts for the assay with 30 pM of target. These values were then used to assess the representative equations. Likewise, the two representative equations previously derived based on the assay in PBS were evaluated using alongside the equations obtained from assay in serum.

The equations were rearranged to solve for the target concentration with regards to the observed SERS intensity. Ideally, the calculated value provided by the representative equations should correspond to the known target concentration associated with either signal intensity. The calculated target concentrations are provided in Table 3 based on the representative equations resulting from linear regression analysis or Hill fit of either the assay in PBS or the assay in bovine serum.

The representative equation obtained using the Hill fit for the assay in bovine serum was the best for predicting target concentration based on the integrated peak intensity. Compared with linear regression analysis, the Hill fit was able to account for the dose-response nature of the sigmoidal curve. However, the use of the Hill equation is limited to the upper and lower bounds, START and END, of the linear portion of the sigmoidal curve. As a result, intensity values outside this range result in an 'undefined' value. The equations calculated using linear regression have no restrictions and can be used with any value. The results also showed the representative equations

calculated based on the assay in PBS were not indicative of the assay in a more complex medium.

SUMMARY

In summary, biomarker detection is a useful tool for diagnosing disease, but its application in clinical settings is limited. In this paper, a SERS-based assay using functionalized metallic nanoparticles labelled with Raman reporter molecules was designed, developed, characterized, and used to target miRNA-17 in solution. The design showed successful detection of miRNA-17 within the range of 1 nM to 1 pM. Linear regression analysis of the data demonstrated statistical significance, and it was used to develop an equation for predicting the target concentration based on the observed relative SERS intensity. Increases in SERS intensity were only observed to be specific to miRNA-17 when compared to 5 different non-complementary strands. The detection of miRNA-17 in this study shows that SERS-based biomarker detection has a high potential to facilitate diagnosis of preeclampsia and potentially other diseases.

Furthermore, our results highlight the value of multiple peak analysis. The capacity of the designed SERS assay for detecting and quantifying miRNA-17 was calculated using the peak area of 5 characteristic peaks of MGITC. While each one of the characteristic peaks was effective in establishing a relationship for quantifying miRNA-17, the combined data demonstrate the consistency of the results obtained. This is important because multiple peaks are rarely simultaneously analysed when evaluating SERS spectra; SERS results are thus often reported based on arbitrary binding ranges and commonly omit calculations of fit and significance. Indeed, differences in SERS spectra analysis and the inconsistency of reported results have led to poor reproducibility. In contrast, multiple peak analysis provides more comprehensive results and comparative determinations of optimal binding ranges, as well as additional insight into the analysis methods of others. As advances in computing emerge, instantaneous multiple peak analysis may efficiently promote the reproducibility of the optical platform. Thus, our designed nanoparticle detection assay for miRNA-17 demonstrates the diagnostic potential for using SERS to create a non-invasive platform for miRNA detection.

Conflicts of interest

There are no conflicts to declare.

Acknowledgements

We acknowledge Dr. Min Hi Park who carried out the qRT-PCR analysis of the bovine serum for this paper. This work was supported, in part, by funding from the Texas A&M Health Sciences Research; Award no. 10072-2, and the Discovery Foundation.

Notes and References

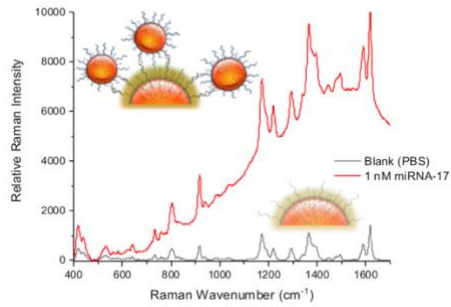
- N. Berkane, P. Liere, J. P. Oudinet, A. Hertig, G. Lefevre, N. Pluchino, M. Schumacher and N. Chabbert-Buffet, *Endocr Rev*, 2017, DOI: 10.1210/er.2016-1065.
- P. von Dadelszen, D. Sawchuck, G. Justus Hofmeyr, L. A. Magee, H. Bracken, M. Mathai, E. Z. Tsigas, K. C. Teela, F. Donnay and J. M. Roberts, *Pregnancy Hypertens*, 2013, **3**, 199-202.
- K. Kanasaki and R. Kalluri, *Kidney Int*, 2009, **76**, 831-837.
- A. S. Lagana, S. G. Vitale, F. Sapia, G. Valenti, F. Corrado, F. Padula, A. M. Rapisarda and R. D'Anna, *J Matern Fetal Neonatal Med*, 2017, DOI: 10.1080/14767058.2017.1296426, 1-5.
- B. M. Sibai, *OBSTETRICS & GYNECOLOGY*, 2003, **102**, 181-192.
- G. D. Baha Sibai and M. Kupferminc, *Lancet*, 2005, **365**, 785-799.
- J. J. van Esch, A. F. van Heijst, A. F. de Haan and O. W. van der Heijden, *J Matern Fetal Neonatal Med*, 2017, DOI: 10.1080/14767058.2016.1263295, 1-6.
- M. Choudhury, H. Li, S. Harshman, M. Freitas and L. Dugoff, *American Journal of Obstetrics and Gynecology*, 2014, **210**.
- C. Salomon, D. Guanzon, K. Scholz-Romero, S. Longo, P. Correa, S. E. Illanes and G. E. Rice, *J Clin Endocrinol Metab*, 2017, **102**, 3182-3194.
- M. Choudhury and J. E. Friedman, *Clin Exp Hypertens*, 2012, **34**, 334-341.
- P. Kumar, Y. Luo, C. Tudela, J. M. Alexander and C. R. Mendelson, *Mol Cell Biol*, 2013, **33**, 1782-1796.
- H. Dong, J. Lei, L. Ding, Y. Wen, H. Ju and X. Zhang, *Chem Rev*, 2013, **113**, 6207-6233.
- J. C. Chuang and P. A. Jones, *Pediatr Res*, 2007, **61**, 24R-29R.
- A. Turchinovich, L. Weiz and B. Burwinkel, *Trends Biochem Sci*, 2012, **37**, 460-465.
- V. S. Nair, C. C. Pritchard, M. Tewari and J. P. Ioannidis, *Am J Epidemiol*, 2014, **180**, 140-152.
- K. Nakamura, K. Sawada, A. Yoshimura, Y. Kinose, E. Nakatsuka and T. Kimura, *Mol Cancer*, 2016, **15**, 48.
- M. de Planell-Saguer and M. C. Rodicio, *Anal Chim Acta*, 2011, **699**, 134-152.
- E. A. Hunt, D. Broyles, T. Head and S. K. Deo, *Annu Rev Anal Chem (Palo Alto Calif)*, 2015, **8**, 217-237.
- MicroRNA Detection and Target Identification* Humana Press, 1 edn., 2017.
- J. A. Weber, D. H. Baxter, S. Zhang, D. Y. Huang, K. H. Huang, M. J. Lee, D. J. Galas and K. Wang, *Clin Chem*, 2010, **56**, 1733-1741.
- Z. Williams, I. Z. Ben-Dov, R. Elias, A. Mihailovic, M. Brown, Z. Rosenwaks and T. Tuschl, *Proc Natl Acad Sci U S A*, 2013, **110**, 4255-4260.
- Circulating microRNAs in Disease Diagnostics and their Potential Biological Relevance*, Springer Basel, 1 edn., 2015.
- K. Hering, D. Cialla, K. Ackermann, T. Dorfer, R. Moller, H. Schneidewind, R. Mattheis, W. Fritzsche, P. Rosch and J. Popp, *Anal Bioanal Chem*, 2008, **390**, 113-124.
- E. Smith and G. Dent, *Modern Raman Spectroscopy – A Practical Approach*, John Wiley & Sons Ltd, 2005.
- K. A. Willets and R. P. Van Duyne, *Annu. Rev. Phys. Chem.*, 2007, **58**, 267-297.
- J. A. Dieringer, A. D. McFarland, N. C. Shah, D. A. Stuart, A. V. Whitney, C. R. Yonzon, M. A. Young, X. Zhang and R. P. Van Duyne, *Faraday Discuss.*, 2006, **132**, 9-26.
- M. Schechinger, H. Marks, A. Locke, M. Choudhury and G. Cote, *J Biomed Opt*, 2018, **23**, 1-11.
- N. Leopold and B. Lendl, *J. Phys. Chem.*, 2003, **107**, 5723-5727.
- D. Graham, D. G. Thompson, W. E. Smith and K. Faulds, *Nat Nanotechnol*, 2008, **3**, 548-551.
- T. Donnelly, W. E. Smith, K. Faulds and D. Graham, *Chem Commun (Camb)*, 2014, **50**, 12907-12910.
- J. N. Anker, W. P. Hall, O. Lyandres, N. C. Shah, J. Zhao and R. P. V. Duyne, *Nature Materials*, 2008, **7**, 442-453.
- K. Faulds, A. Hernandez-Santana and W. E. Smith, in *Spectroscopic Properties of Inorganic and Organometallic Compounds: Techniques, Materials and Applications, Volume 41*, The Royal Society of Chemistry, 2010, vol. 41, pp. 1-21.
- R. A. Alvarez-Puebla, E. Arceo, P. J. G. Goulet, J. J. Garrido and R. F. Aroca, *J. Phys. Chem. B*, 2005, **109**, 3787-3792.
- W. Zhou, Y. F. Tian, B. C. Yin and B. C. Ye, *Anal Chem*, 2017, **89**, 6120-6128.
- M. I. Lopez, I. Ruisanchez and M. P. Callao, *Spectrochim Acta A Mol Biomol Spectrosc*, 2013, **111**, 237-241.
- K. Gracie, E. Correa, S. Mabbott, J. A. Dougan, D. Graham, R. Goodacre and K. Faulds, *Chem. Sci.*, 2014, **5**, 1030-1040.
- H. B. Lueck, D. C. Daniel and J. L. McHale, *J. Raman Spectrosc.*, 1993, **24**, 363-370.
- A. Kamińska, I. Dzieciulewski, J. L. Weyher, J. Waluk, S. Gawinkowski, V. Sashuk, M. Fiałkowski, M. Sawicka, T. Suski, S. Porowski and R. Hołyst, *Journal of Materials Chemistry*, 2011, **21**, 8662.
- C. G. Atkins, K. Buckley, M. W. Blades and R. F. B. Turner, *Appl Spectrosc*, 2017, **71**, 767-793.
- J. Weaver, Y. Shia, D. B. Ness, H. Khurshid and A. Samia, *International Journal on Magnetic Particle Imaging*, 2017, **3**, 4.
- H. Prinz, *J Chem Biol*, 2010, **3**, 37-44.
- Z. Movasaghi, S. Rehman and I. U. Rehman, *Applied Spectroscopy Reviews*, 2007, **42**, 493-541.
- A. C. S. Talari, Z. Movasaghi, S. Rehman and I. U. Rehman, *Applied Spectroscopy Reviews*, 2014, **50**, 46-111.
- M. Lin, L. He, J. Awika, L. Yang, D. R. Ledoux, H. Li and A. Mustapha, *J Food Sci*, 2008, **73**, T129-134.
- R. S. Golightly, W. E. Doering and M. J. Natan, *ACS Nano*, 2009, **3**, 2859-2869.
- H. Zhang, C. Fu, Y. Yi, X. Zhou, C. Zhou, G. Ying, Y. Shen and Y. Zhu, *Analytical Methods*, 2018, **10**, 624-633.
- H. Zhang, Y. Yi, C. Zhou, G. Ying, X. Zhou, C. Fu, Y. Zhu and Y. Shen, *RSC Advances*, 2017, **7**, 52782-52793.

ARTICLE

Analyst

- 1
2
3 48. M. Laguna, M. Holgado, A. L. Hernandez, B. Santamaria, A.
4 Lavin, J. Soria, T. Suarez, C. Bardina, M. Jara, F. J. Sanza and
5 R. Casquel, *Sensors (Basel)*, 2015, **15**, 19819-19829.
6 49. B. Esteban Fernandez de Avila, H. M. Watkins, J. M.
7 Pingarron, K. W. Plaxco, G. Palleschi and F. Ricci, *Anal*
8 *Chem*, 2013, **85**, 6593-6597.
9
10
11
12
13
14
15
16
17
18
19
20
21
22
23
24
25
26
27
28
29
30
31
32
33
34
35
36
37
38
39
40
41
42
43
44
45
46
47
48
49
50
51
52
53
54
55
56
57
58
59
60

TABLE OF CONTENTS IMAGE ENTRY



A SERS sensor was designed as a biomarker based diagnostic tool for preeclampsia with an effective sensing performance.